Modulated electrochemical waves

R. D. Otterstedt, P. J. Plath, and N. I. Jaeger
Institut für Angewandte und Physikalische Chemie, Universität Bremen, FB 2 D-28334 Bremen, Federal Republic of Germany

J. L. Hudson
Department of Chemical Engineering, University of Virginia, Charlottesville, Virginia 22903
(Received 2 February 1996; revised manuscript received 24 May 1996)

Experimental studies have been carried out with ribbon cobalt electrodes in buffered phosphate solutions of different concentration and *p*H under potentiostatic control. Two conditions are investigated. Under oscillatory conditions the system undergoes slow relaxation oscillations between active and passive states, where passivation is due to the presence of a passivating surface film. Oscillations occur in both the total and local currents, although no uniform, spatially independent oscillations are observed. During the activation phase of the oscillations a wave propagates from each end of the electrode toward the center. In the second type of behavior the system has a single, stable passive steady state. Activation past a threshold value of a small region of the ribbon leads to the growth and propagation of the active region. The system is excitable in the sense that a small disturbance, corresponding to a low current or integrated rate of reaction, produces a large excursion before the system returns to its original stable state. Under both types of behavior the leading edge of each wave is visible. The visible leading edge accelerates as it travels along the ribbon; long-range coupling plays a major role in producing this acceleration. When the applied voltage is very close to the Flade potential, the trailing edge of the active region propagates intermittently in the reverse direction, and thus the width of the active region alternately increases and decreases. The velocity of the reverse propagation of the trailing edge is significantly higher than the primary forward velocity of the leading edge. This modulation can be identified as an activation process; it leads to an additional (intermittent) acceleration of the leading edge and to an increase in the total current. [S1063-651X(96)13210-4]

PACS number(s): 47.52.+j

INTRODUCTION

Current oscillations under potentiostatic conditions during anodic dissolution of metals in the transition region between the active and the passive state have been known for a long time, and have been investigated in great detail by many authors [1–3], and references therein]. Oscillations in the cobalt-phosphoric acid system have been reported by Jaeger, Plath, and Quyen [4], and investigated in detail by Pagitsas and Sazou [5,6]. Models of the oscillations during the electrodissolution of iron in the active-passive region have been developed based on the idea that the Flade potential is shifted because of changing *p*H near the surface of the electrode; with the assumption that the surface is uniform [7–10]. However, it is now known that the oscillations are often accompanied by spatiotemporal patterns on the surface.

Lev *et al.* [11] have shown with microreference electrodes that current oscillations on a potentiostatically controlled nickel wire in sulfuric acid in the transpassive region are accompanied by traveling current-density waves. This phenomenon has been modeled recently by the same group [12,13].

Pigeaud and Kirkpatrick [14] investigated the change of reflectivity of an iron disk in sulfuric acid during a current oscillation with an ultramicroscope. The authors observed a brightly reflecting layer during repassivation, growing with decreasing current more or less concentrically from the rim of the disk towards its center, and assumed that it consists of colloidal $Fe(OH)_3$ particles which are located in the beginning of the repassivation process, several microns away from the surface of the electrode, and which later migrate to the surface of the electrode.

Spatiotemporal period doublings and other spatiotemporal bifurcations occurring in the oscillatory range during the electrodissolution of iron in sulfuric acid have been observed by Hudson and co-workers [15,16]; spatiotemporal structures have been observed during cobalt electrodissolution by Otterstedt, Jaeger, and Plath [17].

A model of front and pulse propagation at electrode-electrolyte interfaces has been proposed by Koper and Sluyters [18]. The same authors suggested an improved dissolution-precipitation model with an Ohmic drop for metal electrodissolutions [19].

Otterstedt *et al.* [20] observed accelerating activation fronts in the cobalt-phosphoric acid system. This acceleration occurs both in a bistable region, where a transition from passive to active states is occurring, and also in an oscillatory region, where the activation is one part of the overall oscillatory cycle. Flätgen and Krischer observed accelerating waves in an electrocatalytic reaction, and discussed the importance of the electric field in the electrolyte in producing this acceleration [21,22]. Accelerating waves also occur on iron in sulfuric acid [23].

In this paper we report further on spatiotemporal patterns obtained in the cobalt–buffered phosphoric acid system. The experiments are done on a ribbon electrode which approximates a one-dimensional system.

EXPERIMENTS

The experimental setup is shown in Fig. 1. The working electrode was made from a 50×25-mm cobalt foil of

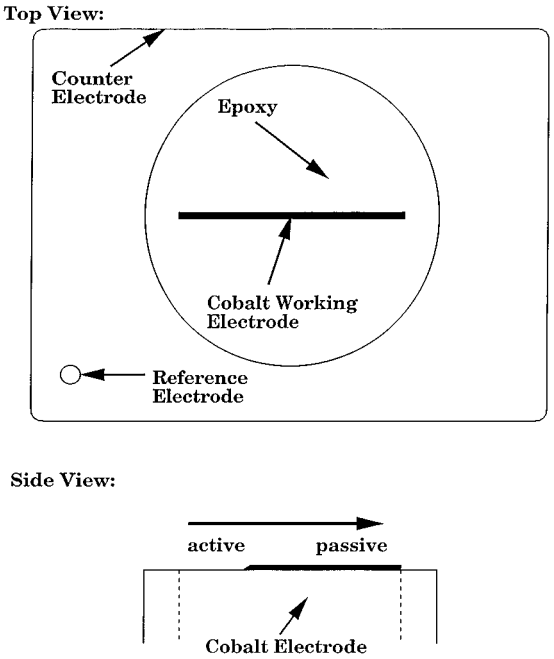

FIG. 1. Top and side views of the experimental setup.

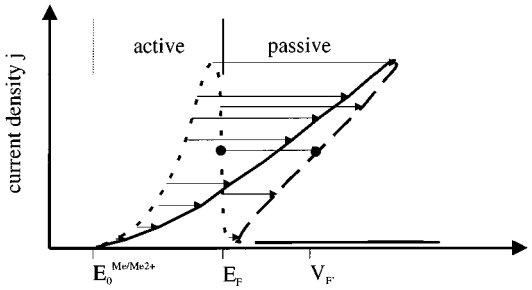

FIG. 2. Schematic drawing of an experimental current-voltage curve showing the active-passive transition at the Flade potential E_F. Solid line, experimental current vs applied potential V_a. Dotted line, current vs electrode potential E. The dashed line represents the active-passive transition not seen in experiment.

0.5-mm thickness (Johnson Matthey), embedded vertically in an epoxy resin such that only the edge of 50×0.5 mm was exposed to the electrolyte. The counterelectrode was made from 2-mm-diameter copper wire, bent to a rectangle of 150 $\times100$ mm, and was located in the same plane as the working electrode. Prior to each experiment, the electrode was sanded wet with grit 400 and grit 2400 sandpaper, and then cleaned in distilled water in an ultrasonic bath. A saturated calomel reference electrode (SCE) was placed in a corner of the counter electrode. The solution level was located 10 mm above the electrode surface. Video images were taken with a video camera and subsequently digitized. Experiments were carried out under potentiostatic control with buffered phosphate solution prepared by dissolving 85% phosphoric acid and dipotassium-hydrogenphosphate in deionized water.

The potential distribution on the ribbon was measured with 12 auxiliary reference electrodes positioned equidistantly in a steel holder 1 mm above the electrode. The signals were recorded with a 12-channel analog-to-digital converter, each channel of which recorded at 100 Hz. Position-time plots of equipotential lines, and cross sections of the latter were made by interpolating linearly between two neighboring positions.

RESULTS

Flade potential

As is discussed below, the modulation is seen at potentials close to the Flade potential. Therefore, an accurate determination of the Flade potential for the cobalt-buffered phosphate system is required.

Figure 2 depicts a schematic drawing of a current-voltage curve showing the active-passive transition at the Flade potential E_F; the curve shows a negative impedance. The solid line shows the experimental current vs the applied voltage V_a; the dashed line represents the unstable branch of the polarization curve which is not seen in the experiment. The idealized curve (dotted line) shows the current vs electrode potential E, which is the applied potential V_a corrected by the Ohmic potential drop in the electrolyte $E=V_a-I$ (total)R, i.e., the potential drop across the electric double layer in front of the electrode and across the passive oxide film. The transition from the active to the passive state occurs when the potential drop across the double layer exceeds the Flade potential ($E>E_F$). In the passive state, E is approximately equal to V_a due to the negligible Ohmic potential drop in the electrolyte. The active state can be reestablished by setting the applied voltage $V_a<E_F$.

The Flade potential was determined in the following manner: the electrode was first passivated by holding it at 1400 mV/SCE, a potential above the Flade potential, for 3 min. The potential was then lowered to a value in the vicinity of the Flade potential. Then the electrode was scratched slightly with a glass rod, and the current was monitored. The current first increases due to the exposed surface of the scratch. When the current decreases afterwards, the chosen potential is considered to be anodic relative to the Flade potential; in the opposite case, it must be cathodic of the Flade potential. Performed iteratively, this method allows the determination of the Flade potential with a precision of about ±5 mV.

Oscillatory region

The system exhibits sustained current oscillations in the 1.0M phosphate buffer of pH 1.67 at an applied potential of 1000 mV/SCE; this potential is 40 mV less than the Flade potential which at this pH is 1040 V/SCE. The oscillations which we are describing do not occur uniformly, i.e., without spatial dependence. Periodic oscillations do occur in the total current, which is, of course, an integral of the current over position. Furthermore, the system oscillates locally as determined by banks of reference electrodes in the solution near the electrode surface. As far as we know, however, the system does not have an oscillatory state in which variables depend only on time and not on position. This type of behavior is likely common in the oscillatory dissolution of metals. In many experiments previously reported, only the integrated behavior, the total current, has been determined [3]. We note that, in the oscillations reported in this paper, the period depends on the system geometry; the frequency increases with decreasing electrode size for two reasons: (a)

the time required for the waves to propagate across the electrode is greater for a larger electrode, and (b) the total current with a larger electrode is greater which moves the potential drop across the double layer farther into the cathodic region which slows the repassivation.

The experiments are carried out by first holding the system at a potential $E=1400$ mV, which is anodic to the Flade potential; at this condition the system is in the passive region, so that a film develops on the surface. The potential is then reduced to $E=1000$ mV, which is cathodic with respect to the Flade potential. Under these conditions, autonomous oscillations will eventually occur, but the transient is slow because of the presence of the film. In order to speed up the transient process, the initially passive electrode is scratched at one end, as described above. This small active region immediately begins to move toward the center of the ribbon; another active region forms (without scratching) at the other end of the electrode and also propagates toward the center, although this second region lags the first. The leading edges of these two active regions are visible. The leading edges of the two regions meet, and annihilation occurs. After a short delay, two new active regions, one from each end, again propagate toward the center. After a couple of oscillations the system oscillates symmetrically, that is, waves propagate from each end, meet in the center, and then the process is repeated.

We first consider an example of oscillatory behavior under conditions in which modulation does not occur; i.e., we consider a case in which the applied potential is not close to the Flade potential. A single autonomous current oscillation after transients have died down can be seen in Fig. 3. The current is shown in Fig. 3(a). The amplitude of each oscillation is approximately 130 mA. The positions of the leading edges of the propagating waves were obtained from the digitized video images; they can be seen in Fig. 3(b). The leading edges of the waves meet at the center of the electrode in approximately 0.5 s. An acceleration can be inferred from Fig. 3(b), since the velocity is increasing; this is consistent with the increasing current seen in Fig. 3(a). More information on acceleration of fronts and waves in this electrochemical system can be found in [20].

Active regions thus propagate through a previously passive medium. The width of each region is not constant, but rather increases monotonically. The repassivation has a slower time scale than the activation, and the repassivation at the tail of the active region moves more slowly than the leading edge. Because of this, the current rises as can be seen in Fig. 3(a). We note, furthermore, that under the conditions of Fig. 3 the width of the active region is relatively large so that the repassivation area behind the active pulse cannot be distinctively seen before the leading edges meet in the center of the electrode. The width of the active regions decreases as the potential is brought closer to the Flade potential; thus for somewhat higher potentials the width is smaller, and a pair of active regions can be more clearly seen propagating from the edges of the electrode toward the center.

At an even higher potential, only slightly cathodic to the Flade potential, the system is again in the oscillatory region; in this region the widths of the active regions are very small, and modulation occurs. An example of the current under such conditions is shown in Fig. 4(a), and the position of the

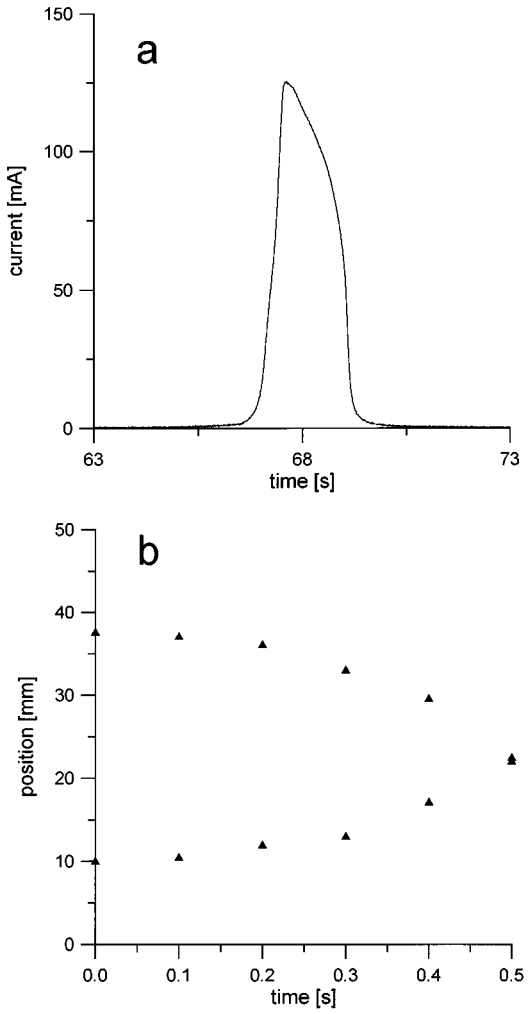

FIG. 3. (a) Single autonomous oscillation without modulation: 1.0*M*, phosphate buffer; pH$=1.67$; applied potential 1000 mV/SCE. (a) Current vs time. (b) Position of the leading edge of the activation vs time.

propagating leading edge in Fig. 4(b). The oscillation shown in Fig. 4 is the first oscillation observed after the oscillations are initiated by scratching; this first oscillation is considered because the visible leading edges are clearer and easier to detect than those which occur later after transients have died down. The active region again progresses from one end of the electrode toward the other. As the active region propagates, the trailing edge itself, in an intermittent or propagating manner, accelerates in the reverse direction into the repassivated region. This trailing edge, when accelerating in the reverse direction, is also visible. The velocity of the trailing edge (in the reverse direction) is much greater than the velocity of the leading edge in the forward direction. However, the trailing edge does not propagate completely to the end of the electrode, but rather appears to die out before another modulation occurs. Several expansions and contractions of the active region width can occur as the wave propagates across the electrode. Furthermore, as shall be seen below, as acceleration of the trailing edge in the reverse direction occurs, there is an increased acceleration of the leading edge in the forward direction.

This modulation occurs with the applied voltage very close (within a few millivolts), but cathodic, to the Flade

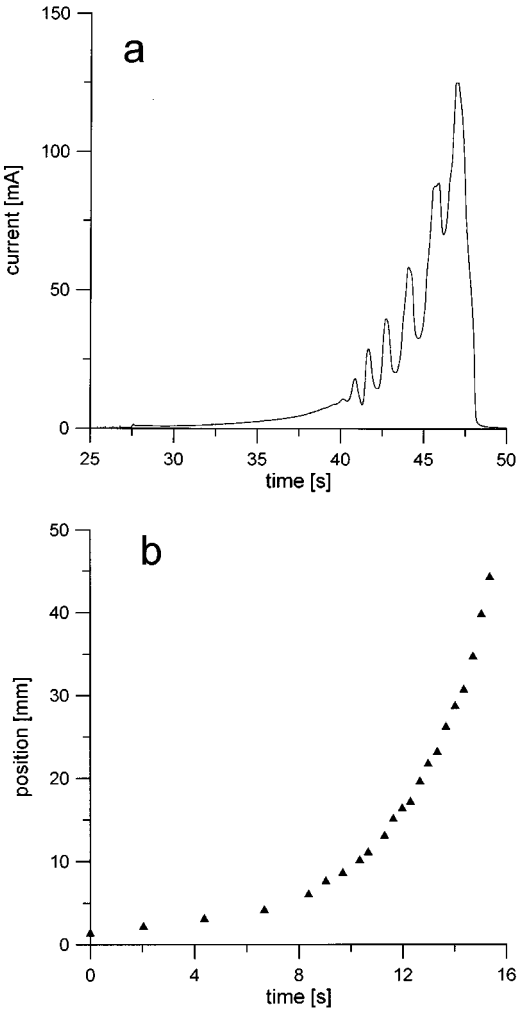

FIG. 4. Single oscillation with modulation; the oscillation shown is the first after activation. 1.25*M*, phosphate buffer; *p*H =1.5; applied potential, 1050 mV/SCE. (a) Current vs time. (b) Position of the leading edge of the activation vs time.

potential. The phenomenon could be most clearly observed in 1.25*M* phosphate buffer of *p*H 1.50. In this solution the Flade potential was determined to be 1065 mV/SCE. The electrode was passivated for 150 s at 1400 mV/SCE; then the applied potential was stepped down. It was found that a potential of 1050 mV, just below the Flade potential in this solution, gave optimum results. The current is shown in Fig. 4(a). The modulation can be clearly seen in the shape of the current vs time behavior. The position of the leading edge of the propagating modulated wave is shown in Fig. 4(b). The position of the leading edge increases monotonically with time. There is again an upward concave shape denoting acceleration of the leading edge. Note that the period of the oscillation increases considerably, almost by an order of magnitude, as the applied potential is moved close to the Flade potential; this can be seen by comparing Figs. 3(b) and 4(b).

The velocity of the leading edge of the pulse is determined from the data shown in Fig. 4(b) by taking the differences of successive position points; this yields curve 2 shown in Fig. 5. The velocity is small, and almost constant, for the early portion, up to about 10 s. Then the velocity

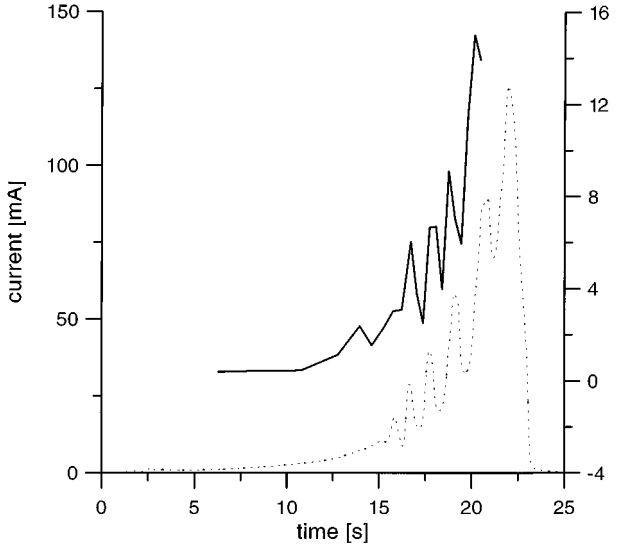

FIG. 5. Single oscillation with modulation. Same conditions as Fig. 4. (1) Current. (2) Velocity of the leading edge of the pulse obtained from Fig. 4(b).

begins to increase and shows the same modulation as the current in Fig. 4(a), which is again depicted in Fig. 5 as curve 1. The modulation of the current parallels that of the velocity, i.e., a local maximum in current corresponds to a local maximum in the velocity.

The potential in the electrolyte at a distance of 1 mm from the ribbon electrode was measured with a bank of 12 reference electrodes. By means of a linear interpolation between each pair of electrodes, the potential field along the ribbon was determined as a function of time. Equipotential lines are

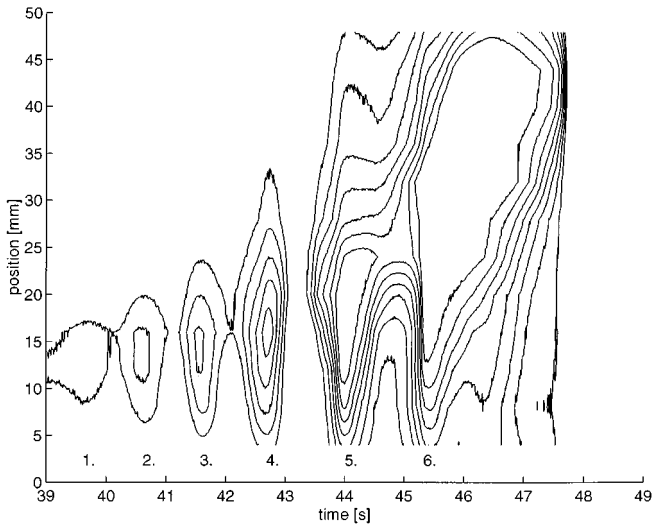

FIG. 6. Position time plot of selected equipotential lines as derived from the signals obtained from 12 auxiliary reference electrodes positioned equidistantly along the ribbon. Time denotes the time elapsed after stepping the potential down from 1200 to 1056 mV/SCE, and placing the drop of acid on the ribbon at position 0 mm. The numbers denote the maxima in the corresponding current-time curve (see Fig. 7). The outside equipotential lines correspond to a potential of 300 mV cathodic, with respect to the applied potential of 1056 mV/SCE. Subsequent lines are 50 mV, apart.

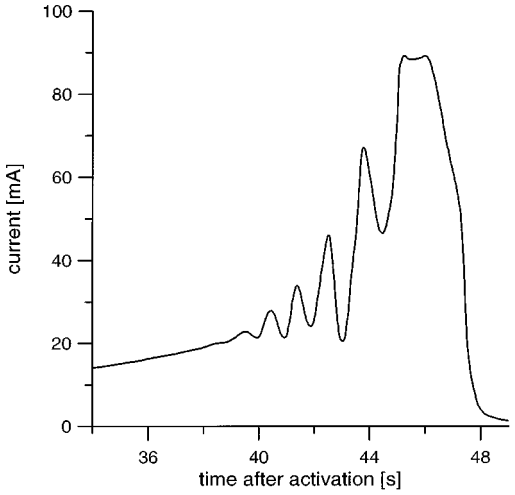

FIG. 7. Current-time curve with modulation following the initiation of activation: 1.25*M* phosphate buffer, *p*H=1.50, applied potential 1056 mV/SCE. The system is oscillatory, with a period of 90 s.

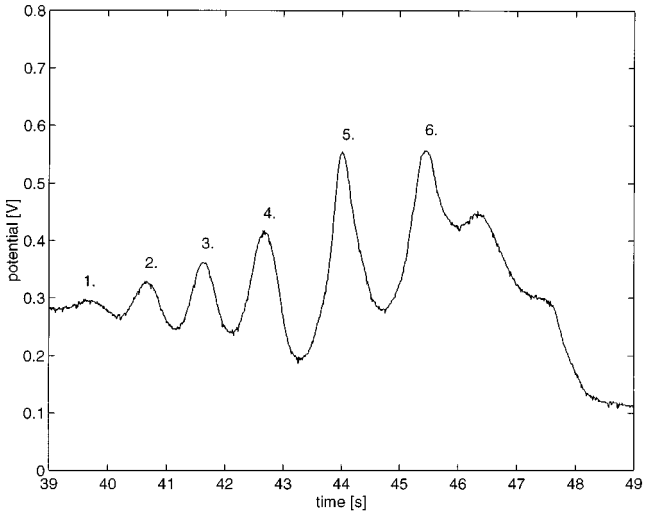

FIG. 8. Potential time curve at the position 8 mm on the ribbon (cross section of Fig. 6). The numbers denote the maxima in the corresponding current-time curve (Fig. 7).

shown in time-distance space in Fig. 6 for an experiment done in the oscillatory region where modulation occurs. Although the experimental conditions are slightly different than those of Fig. 5, the two cases show similar behavior. (For Figs. 6–9, an auxiliary external resistance of 1.1 Ω was used. This resistance was used to make the maxima and minima in the current-time curves more pronounced. All the phenomena described, both in the oscillatory and excitable regions, can be obtained with and without the external resistance.) The current-time curve for the experiment of Fig. 6 is shown in Fig. 7.

Figures 6 and 7 correspond to the first oscillation after the first wave is initiated, and the time indicated is the time after this initiation. After a few oscillations the system reaches a stationary oscillatory state. The potential of the electrode is 1056 mV/SCE. In Fig. 6, the outer equipotential line denotes a potential of 300 mV cathodic to (less than) the electrode potential. Successive lines are drawn for 50-mV increments, i.e., the next line denotes a potential of 350 mV cathodic. The lowest potential line shown is 650 mV cathodic, which can be seen in the region between approximately 45 and 47 s and a position between approximately 13 and 48 mm. There are six current maxima in Fig. 7, and these correspond to the six indicated regions of Fig. 6. In each of these regions there is a potential plateau; the largest of these plateaus corresponds to the sixth current maximum.

The leading edge of the active region moves at first slowly, then more quickly as it progresses along the ribbon. During this progression six distinct modulations occur, i.e., the trailing edge propagates six times in the reverse direction. The first four of these modulations occur when the leading edge is still moving relatively slowly; the trailing edge propagates only a short distance in the reverse direction in these four cases. During the fifth and sixth modulations the trailing edge propagates rapidly backwards along the ribbon, i.e., in a direction opposite to that of the leading edge. These trailing edges move much more rapidly than the leading edge. This can be seen in part by observing the increased width of the low potential plateaus in Fig. 6, i.e., the plateau for event 6 is larger than that for event 5, and both are larger than the others.

The potential in the electrolyte at a given position along the ribbon (8 mm) is shown in Fig. 8. This figure is a cross section of Fig. 6. Again, the oscillations in the potential can be seen. Note that the effect of the modulation is felt at the distance of 8 mm, even though the leading edge is well past this position. This is because of the strong long-range coupling in this system, i.e., changes at one location are felt nonlocally.

Stable steady state

At applied potentials anodic (positive) to the Flade potential the system is in a stable, passive state in which no oscillations occur. Very close to the Flade potential the system exhibits excitable characteristics. No uniform (spatially independent) excitability has been observed, and it is likely not possible to excite the entire system uniformly. Nevertheless, the system can be excited in the following sense: we produce a local disturbance (an active area) by removing the passive film at one location. If this disturbance is very small, the system returns immediately to the original stable passive state. If the disturbance is somewhat larger, i.e., above a threshold, the active region expands and travels along the electrode. The current increases to a value much larger than the value produced by the disturbance. When the active area reaches the end or ends of the electrode, the current drops to its original value. The current versus time dependence resembles that of a classical, spatially independent excitable system which has been disturbed past a threshold. The electrochemical system can be said to exhibit spatiotemporal excitability.

The experiments are done as follows: the ribbon electrode is originally in the passive, stable state at an applied potential which is slightly anodic to the Flade potential. A cobalt wire of diameter 1 mm, of which normally only the end is bare, is placed against the passive ribbon. Since the wire has no protective film, an oxidation reaction occurs on it immediately after its potential is brought to that of the ribbon. Oxidation

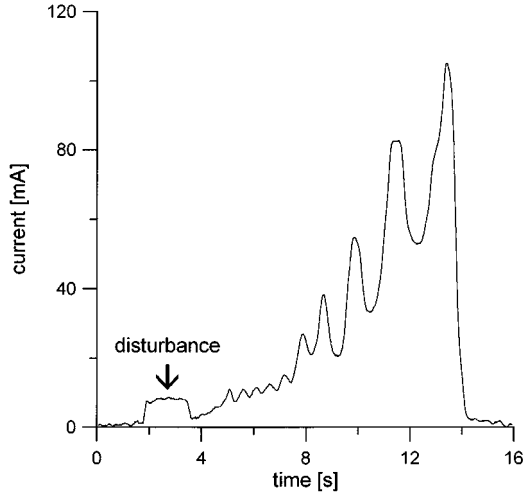

FIG. 9. Current-time curve with modulation following initiation of activation in the passive region: 1.25*M* phosphate buffer, *p*H =1.67, applied potential 1150 mV/SCE. Passivation for 15 s. Disturbance at the end of the ribbon.

on the wire causes a corresponding reduction of the ribbon electrode and this reduction removes locally a portion of the protective film. A small active region has thus been produced on the ribbon electrode. After initiation, the single active region travels along the ribbon, reaches the end or ends, and the system returns to the original passive state. Since these experiments are done at potentials close to the Flade potential, the width of the active region is relatively small as discussed above, and modulation usually occurs; this modulation is similar to that described above for the oscillatory regime.

A current-time curve is shown in Fig. 9. This experiment was done by passivating the ribbon for 15 s, and then disturbing the ribbon with the cobalt wire at a position very close to one end. The ribbon is initially passive and the current is low, as can be seen in the figure. At time approximately $t=33.5$ s, the disturbance is imposed and held for about 2.5 s. The wire is then removed, and the current falls slightly at $t=36$ s. The disturbance is, however, large enough that an active region has been produced which propagates toward the other end of the wire. The active region expands as it travels, since the activation is faster than the passivation, and the current rises. The active region grows and shrinks (breathes), as seen above in the oscillatory region and a modulation of the current occurs. The active region reaches the end of the wire at $t=46$ s, and the current falls to a very low value and remains there.

The disturbances can also be imposed in the middle of the ribbon. In this case the edges of the active region move in both directions. As the two active regions move toward the ends of the ribbon, the region in the center begins to repassivate. The active regions again grow since the passivation occurs more slowly than the activation; the current rises as seen above, and the current then drops after the active regions reach the ends of the ribbon.

Three examples of activation in the middle are shown in Fig. 10. In each case the ribbon was first passivated for 30 s at 1150 mV. In the experiment shown in Fig. 10(a), the ribbon was activated with the same cobalt wire used in the

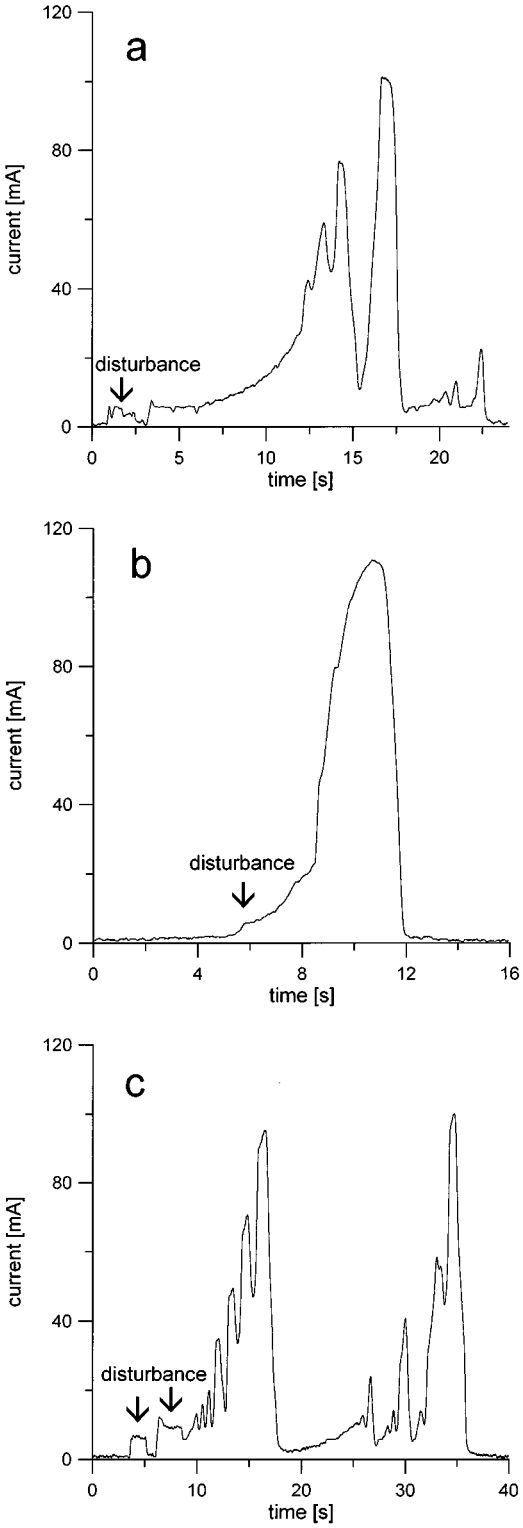

FIG. 10. Current-time curve following activation in the passive region. Passivation for 30 s. *p*H=1.67. 1.25*M* is the phosphate buffer, and the potential is 1150 mV. The disturbance is in the middle of the ribbon. (a) Small disturbance. (b) Larger disturbance. (c) With added external resistance $R=2\ \Omega$.

experiment of Fig. 9. In Fig. 10(a), the disturbance was imposed beginning at time 1 s for about 2.5 s. Note that the current again rises during the disturbance, and then falls after the wire is removed. The current then rises, and modulation occurs as the width of the active region grows and shrinks.

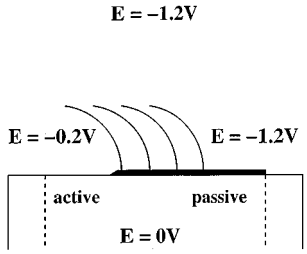

FIG. 11. Schematic of the accelerating leading edge.

The experiment shown in Fig. 10(b) is done in a similar manner, except that the disturbance is greater, i.e., it was made with a cobalt wire whose exposed area was larger, about 4.0 mm^2 as opposed to about 1 mm^2 as in Fig. 10(a). Since the disturbance is greater, the active area is wider, the reformation of the passive region behind the wave is hindered, and much less backpropagation of the trailing edge occurs. In Fig. 10(b) only very slight modulation can be seen. The experiment of Fig. 10(c) was done with the same cobalt wire as in Fig. 10(a). However, in Fig. 10(c) a very small external resistance was added to the system. (In general, the addition of an external resistance enhances the disturbances; therefore, the resistance was added to make the following result more evident.) The middle of the ribbon was disturbed at time 4 s. This disturbance was not large enough to cause the formation of an active region which could propagate. A second disturbance was then imposed at a time 6 s; in the second disturbance, the wire was held on the electrode for a longer time, and the disturbance was therefore greater. After the second disturbance, an active region was formed which propagated in the two directions. These active regions reached the ends of the electrode at a time 18 s, and the current fell. As can be seen, modulation of the current and breathing of the active region occurred. After the active regions reached the ends of the electrode, one end remained slightly active, and the active region propagated backwards in the opposite direction, traversed the entire electrode, and reached the other end, at which time the electrode returned to its original passive, stable state at a time 36 s.

DISCUSSION

The electrochemical system exhibits two interesting characteristics, viz. acceleration and modulation; we discuss these briefly in turn.

Consider first the acceleration. A schematic of an activation front is shown in Fig. 11. The sharp edge marks the border between the passive oxide and the active area which expands from left to right. Long-range coupling plays a major role in the acceleration of waves and fronts. The long-range coupling is caused by the electric field. The field lines are shown in Fig. 11. In the active region there is a relatively small potential gradient across the electric double layer (0.2 V in the sketch) and a larger Ohmic potential drop (1.0 V). In the passive region, there is a potential drop of 1.2 V (the entire applied voltage) across the double layer and the protective film. The potentials given are measured relative to ground. There is, of course, a smooth transition in the electrolyte. Migration currents flow parallel to the surface. The passive film near the edge of the active region is cathodic to the Flade potential, and therefore electrodissolution occurs.

In electrochemical systems there is coupling through the electric field causing migration currents, as was pointed out by Franck and Meunier [24]. This is a nonlocal, or long-range, coupling which exists in addition to the diffusive coupling. Because the potential is not uniform throughout the electrolyte, and therefore the coupling can decrease with position, the coupling is termed long-range rather than global. Flätgen and Krischer [21,22] showed how nonlocal coupling can cause acceleration of electrochemical waves. Bell, Jaeger, and Hudson [25] showed that migration currents can play a major role in the coupling between two oscillating cobalt electrodes. Sevcikova, Marek, and Müller [26] investigated the influence of an electric field on the velocity and direction of wave propagation in the Belousov-Zhabotinskii reaction, and showed the existence of wave splitting.

The concept of nonlocal, or global, coupling is not limited to electrochemical systems. Middya and co-workers [27,28] showed how a global interaction caused by an integral constraint leads to spatiotemporal patterns. The effect of global coupling on spatiotemporal patterns was investigated experimentally and in a mathematical model by Veser *et al.* [29] and Mertens, Imbihl, and Mikhalov [30].

The long-range coupling certainly has an important effect on the acceleration seen in the metal electrodissolution being discussed. However, there is another important feature of this system. The rate of dissolution of the passive film is an exponential function of the difference of the electrode potential relative to the Flade potential in the cathodic direction [20]. As the active area expands, the total current increases; therefore the Ohmic potential drop in the electrolyte also increases. This increase shifts the potentials farther into the cathodic region, and increases the rate of electrodissolution of the oxide film. The movement of the potentials into the cathodic region and the exponential dependency of the rate of dissolution on the potential lead to an additional acceleration. The system has positive feedback analogous to an autocatalysis.

The system exhibits a type of excitability which is spatiotemporal in nature. After a small, local disturbance, the system returns directly to the steady state. With a somewhat greater disturbance, a propagating active area is formed which grows rapidly, causing a large excursion of the current before the system returns to its original passive stable steady state.

When the applied potential is very close to the Flade potential, modulation is observed in both the oscillatory and excitable regions. In order to explain this phenomenon, reference is again made to the pH dependence of the Flade potential. The Flade potential of a metal depends on the pH of the solution according to the relationship: $E_F = E_{0,\mathrm{metal}} + RT/nF \ln a_{H^+}^{\nu}$, where ν is the stoichiometric coefficient and n the number of electrons in the electrode reaction [31,32]. As the surface is activated, hydrogen ions migrate away from the active surface toward the counter electrode. This leads to a shift of the Flade potential to the left (lower potential). If the Flade potential is shifted to the left of the applied potential, the surface begins to repassivate after the leading edge has passed. When the applied potential is very near to—and either cathodic to or anodic to—the

Flade potential, the activation front is slow, and the active area behind the wave can repassivate at approximately the time scale of the propagation of the leading edge. The passivating film will be very thin, and shortly after it has been formed it will begin to be removed by the same mechanism which drives the primary leading edge. (Here we ignore the hydrogen ions formed during the passivation of the metal.)

Observations with a series of closely spaced reference electrodes (Fig. 6) clearly show that the backward movement of the trailing edge is also a propagation of an active region into a passive one, similar to that which occurs at the leading edge. The velocity of the trailing edge (in the reverse direction) is about an order of magnitude greater than that of the leading edge. When the modulation occurs, both the total current and the velocity of the leading edge of the active region increase.

A somewhat different phenomenon, backfiring of pulses has been shown to exist in a surface reaction model for CO oxidation by Bär *et al.* [33]. Their model is an activator-inhibitor system, which for some parameter values simulates an excitable medium. Under some conditions an increase in a parameter caused a decrease in the size of the refractory zone behind pulses, and at a critical value of this parameter reexcitation occurred. The reexcitation led to new pulses.

The modulated waves in the electrochemical system appear to have similar characteristics with the modulated traveling waves seen by Bayliss, Matkowsky, and Rieke in cellular flames [34]; Brown and Kevrekidis considered modulated traveling waves in the Kuramoto-Sivashinsky equation [35].

In our work the principal parameter is the applied potential of the electrode. As this parameter is moved closer to a critical value, the Flade potential, the velocity of the leading edge of the active region decreases. This slower motion allows for a repassivation in back of the region, in part through the transport of hydrogen ions away from the electrode surface. As the velocity becomes small, conditions for activation in the reverse direction become favorable and modulation occurs.

ACKNOWLEDGMENTS

The work was supported in part by grants from the National Science Foundation, the Deutsche Forschungsgemeinschaft (JA 346-16-1), and NATO. We thank Yannis Kevrekidis and Bernie Matkowsky for helpful discussions.

[1] J. Woijtowicz, in *Modern Aspects of Electrochemistry*, edited by J. OM. Bockris and B. E. Conway (Plenum, New York, 1973), Vol. 9, p. 47.
[2] J. L. Hudson and M. R. Bassett, Rev. Chem. Eng. **7**, 109 (1991).
[3] J. L. Hudson and T. T. Tsotsis, Chem. Eng. Sci. **49**, 1493 (1994).
[4] N. I. Jaeger, P. J. Plath, and N. Q. Quyen, in Temporal Order, edited by L. Rensing and N. I. Jaeger [Spring. Ser. Synerg. **29**, 103 (1984)].
[5] M. Pagitsas and D. Sazou, J. Electroanal. Chem. **81**, 334 (1992).
[6] D. Sazou and M. Pagitsas, J. Electroanal. Chem. **332**, 247 (1992).
[7] U. F. Franck and R. FitzHugh, Z. Elektrochem. **65**, 156 (1961).
[8] A. J. Pearlstein and J. A. Johnson, J. Electrochem. Soc. **136**, 1290 (1989).
[9] Y. Wang, J. L. Hudson, and N. I. Jaeger, J. Electrochem. Soc. **137**, 485 (1990).
[10] M. Pagitsas and D. Sazou, Electrochim. Acta **36**, 1301 (1991).
[11] O. Lev, M. Sheintuch, L. M. Pismen, and Ch. Yarnitzky, Nature **336**, 458 (1988).
[12] D. Haim, O. Lev, L. M. Pismen, and M. J. Sheintuch, J. Phys. Chem. **96**, 2676 (1992).
[13] D. Haim, O. Lev, L. M. Pismen, and M. J. Sheintuch, Chem. Eng. Sci. **47**, 3907 (1992).
[14] A. Pigeaud and H. B. Kirkpatrick, Corrosion **25**, 209 (1969).
[15] J. L. Hudson, J. Tabora, K. Krischer, and I. G. Kevrekidis, Phys. Lett. A **179**, 355 (1994).
[16] J. C. Sayer and J. L. Hudson, Ind. Eng. Chem. Res. **34**, 3246 (1995).
[17] R. D. Otterstedt, N. I. Jaeger, and P. J. Plath, Int. J. Bifurc. Chaos **4**, 1265 (1994).
[18] M. T. M. Koper and J. H. Sluyters, Electrochim. Acta **38**, 1535 (1993).
[19] M. T. M. Koper and J. H. Sluyters, J. Electroanal. Chem. **347**, 31 (1993).
[20] R. D. Otterstedt, P. J. Plath, N. I. Jaeger, J. C. Sayer, and J. L. Hudson, Chem. Eng. Sci. **51**, 1747 (1996).
[21] G. Flätgen and K. Krischer, Phys. Rev. E **51**, 3997 (1995).
[22] G. Flätgen and K. Krischer, J. Chem. Phys. (to be published).
[23] B. G. Sullivan, thesis, University of Virginia, Charlottesville, 1990.
[24] U. F. Franck and L. Meunier, Z. Naturforsch. **86**, 396 (1953).
[25] J. C. Bell, N. I. Jaeger, and J. L. Hudson, J. Phys. Chem. **96**, 8671 (1992).
[26] H. Sevcikova, M. Marek, and S. C. Müller, Science **257**, 951 (1992).
[27] U. Middya, M. Sheintuch, M. D. Graham, and D. Luss, Physica D **63**, 393 (1993).
[28] U. Middya and D. Luss, J. Chem. Phys. **100**, 6386 (1994).
[29] G. Veser, F. Mertens, A. S. Mikhailov, and R. Imbihl, Phys. Rev. Lett. **71**, 935 (1993).
[30] F. Mertens, R. Imbihl, and A. S. Mikhailov, J. Chem. Phys. **101**, 9903 (1994).
[31] K. J. Vetter, *Elektrochemische Kinetik* (Springer-Verlag, Berlin, 1961), p. 603.
[32] K. E. Heusler, Corros. Sci. **6**, 183 (1965).
[33] M. Bär, M. Hildebrandt, M. Eiswirth, M. Falcke, H. Engel, and G. Ertl, Chaos **4**, 499 (1994).
[34] A. Bayliss, B. J. Matkowsky, and H. Rieke, Physica D **74**, 1 (1994).
[35] H. S. Brown and I. G. Kevrekidis, Fields Institute Commun. **5**, 45 (1996).